Pacheco, M., Jurado-Sánchez, B. and Escarpa, A. (2018) 'Sensitive Monitoring of Enterobacterial Contamination of Food Using Self-Propelled Janus Microsensors', Analytical chemistry (Washington), 90(4), pp. 2912–2917.

Available at https://doi.org/10.1021/acs.analchem.7b05209

SENSITIVE MONITORING OF ENTEROBACTERIAL CONTAMINATION OF FOOD USING SELF-PROPELLED JANUS MICROSENSORS

M. Pacheco,[‡] B. Jurado-Sánchez,[‡,∥*] A. Escarpa[‡,∥*]

[‡]Department of Analytical Chemistry, Physical Chemistry and Chemical Engineering, University of Alcala, Alcala de Henares E-28871, Madrid, Spain. E-mail: beatriz.jurado@uah.es; alberto.escarpa@uah.es (Tel.: +34 91 8854995).

[∥]Chemical Research Institute "Andrés M. del Río", University of Alcala, Alcala de Henares E-28871, Madrid, Spain.

ABSTRACT: Food poisoning caused by bacteria is a major cause of disease and death worldwide. Herein we describe the use of Janus micromotors as mobile sensors for the detection of toxins released by enterobacteria as indicators of food contamination. The micromotors are prepared by a pickering emulsion approach and rely on the simultaneous encapsulation of platinum nanoparticles -for enhanced bubble-propulsion- and receptor-functionalized quantum dots (QDs) for selective binding with the 3-deoxy-d-manno-oct-2-ulosonic acid target in the endotoxin molecule. Lipopolysaccharides (LPS) from *Salmonella enterica* were used as target endotoxins, which upon interaction with the QDs induce a rapid quenching of the native fluorescence of the micromotors in a concentration-dependent manner. The micromotor assay can readily detect concentrations as low as 0.07 ng mL^{-1} of endotoxin, which is far below the level considered toxic to humans (275 µg mL^{-1}). Micromotors have been successfully applied for the detection of *Salmonella toxin* in food samples in 15 minutes compared to several hours required by existing *Gold Standard* method. Such ultrafast and reliable approach holds considerable promise for food contamination screening while awaiting the results of bacterial cultures in a myriad of food safety and security defense applications.

Food safety is a global issue with a great socio-economic impact worldwide. Primary foodborne pathogens including *Campylobacter*, *Salmonella*, *Listeria monocytogenes*, and *Escherichia Coli* are the subject of intense research by the scientific community and international agencies.[1-2] On particular, *Salmonella* infects an estimated of 1.4 million people in the United States and tens of millions worldwide, accounting for 100.000 deaths every year.[3-5] Subtle and early detection is essential to control potential human poisoning and to prevent the spread of the infection. Bacteria culture is considered as the gold standard, but requires at least 5 days to obtain reliable results. Immunological and PCR-based methods are labor-intensive and prone to false negatives.[6-8] Affinity-based biosensors with electrochemical, optical and impedimetric detection have been widely explored for direct foodborne bacteria detection.[4, 9-10] While some of these procedures have become commercially available, more improvements are needed to meet all the requirements for fast response. This demands for more efficient and fast protocols for *"on-time"* detection of enterobacterial contamination. In a previous work, we demonstrate for the first time the encapsulation of graphene quantum dots (GQDs) as sensing probes into Janus micromotors and prove the concept using *Escherichia Coli* lipopolysaccharides (LPS) as model toxin.[11] Yet, the relatively high limits of detection obtained prevent its practical utility and more studies are needed. Since enterobacteria contamination results in the release of endotoxins (such as *Salmonella* endotoxin) herein we hypothesize that QDs functionalized Janus micromotors can be applied as a fast, simple and sensitive test for enterobacterial contamination of food.

Self-propelled micromotors, capable of converting energy into movement and forces, have revolutionized sensing technology, leading to new *'on-the-fly'* detection schemes along with higher efficiency, shorter times, no sample preparation and potentially lower costs.[12-18] As promising examples, micromotors engineered with conventional fluorescent dyes or nanoparticles such as quantum dots have been used for chemical weapons and heavy metal threats detection, with real-time fluorescent visualization of the analyte recognition event.[11, 19-23] Real-time analytical measurements *"on-site"* can thus be performed, either near chemical spots or directly in living cells, to report on the local concentration of the target analyte by changes in their optical properties.[18, 24-26] Such new "nanoscale" tools also allow for the design of field-portable analytical systems. Yet, few reports deal with the use of micromotor for food safety applications. In this context, our group have reported the use of galactosidase modified micromotors for lactose removal and graphene micromotors for mycotoxin detection.[27,28] Also, Schmidt group reported a graphene-composite-sodium borohydride micromotor for value-added product synthesis.[29] Yet, to the best of our knowledge, this is the first time that Janus micromotors are used in food control applications for deadly toxins detection.

The micromotor-based mobile sensing strategy reported here allows for fast monitoring of enterobacterial contamination in food through detection of endotoxins. Such compounds are constituent of the outer membrane of the cell wall of gram-negative bacteria, and are released in small amounts during its growing, and promptly after contamination.[30] The micromotors are synthetized via a Pickering emulsion approach, and rely on the simultaneous encapsulation of nanoparticles -for enhanced bubble

propulsion- and receptor-functionalized quantum dots for selective binding to 3-deoxy-d-manno-oct-2-ulosonic acid (KDO), a characteristic component of the endotoxin structure. *Salmonella enterica* was used as main enterobacterial indicator, which upon interaction with the quantum dots induce a rapid quenching of the native fluorescence of the micromotors in a concentration-dependent manner. Main novelty here is the use, for the first time, of Janus micromotors for food safety applications. In the following sections, we will demonstrate the feasibility of our monitoring strategy for the sensitive (ng mL^{-1} levels) and selective detection of the target toxin in raw, viscous food samples in 15 minutes compared to several hours required by existing methods.[30] The new strategy holds considerable promise for ultrafast detection of food contamination while awaiting the results of bacterial cultures and, most importantly, is particularly valuable when contamination is suspected but bacteriological methods fail to recover the organism. In addition, endotoxin detection is important since it can also cause watery diarrhea or dysentery, a more severe infection caused by *Salmonella*.

EXPERIMENTAL SECTION

Reagents and equipment. *Salmonella enterica* serotype enteritidis (cat. L7770), D-fructose (cat. F0127), glucose (cat. G5767) and galactose (cat. G0625) were obtained from Sigma-Aldrich. Sodium dodecyl sulfate (cat. 71727) was supplied by Merck (Germany). Milk and egg samples were obtained from local supermarkets. An inverted optical microscope (Nikon Eclipse Instrument Inc. TiS/L100), coupled with 10X and 40X objectives, and a Hamamatsu digital camera C11440 and NIS Elements AR 3.2 software, were used for capturing movies at a rate of 25 frames per second. The speed of the micromotors was tracked using a NIS Elements tracking module. The microscope includes an Epi-fluorescence attachment with a UV-2E/C (DAPI) filter cube. Raman spectra was obtained using a micro-Raman system (Witec alpha-300R) with 100x objective lens (NA=0,95) and 1 mW the incident laser power.

Graphene quantum dots synthesis and characterization. The quantum dots were prepared by direct pyrolysis of citric acid and dispersion in alkaline solutions. In brief, 1.5 g of citric acid (cat. 251275) were heated to 150 °C using a heating mantle for 10 min until the formation of an orange liquid. Next, as-obtained liquid was added drop by drop into a 50 mL NaOH solution (0.1 M) and the pH of the resulting solution was adjusted to 7.0 to trigger the dispersion of the GQDs. For functionalization, 1 mL of GQDs solution was mixed with 1 mL of PBS buffer (0.1 M, pH 7.4), 12 mg of 3-Aminophenylboronic acid monohydrate (cat. 287512) and 16 mg of N-(3-Dimethylaminopropyl)-N-ethylcarbodiimide (cat. 39391) and mixed in a vortex for 3 h. The resulting quantum dots have a round morphology with an average particle size of ~3 nm (by atomic force microscopy) and exhibit strong fluorescence emission at 470 nm after excitation at 360 nm (see Figure S1).

Platinum nanoparticles synthesis. Platinum nanoparticles (average particle size 100 nm) were obtained by chemical reduction of chloroplatinic acid (cat. 398322) with hydrazine (30% in H_2O_2, cat. 309400) at 25 ºC and pH 10. In a typical procedure, 250 mg of H_2PtCl_6 were dissolved in 1 mL of NaOH (12 M) and stirred by magnetic stirrer. The reduction of the metal ions was accomplished by adding hydrazine solution as reducing agent. The resulting precipitate, which contains the platinum nanoparticles, was separated by centrifugation (3000 rpm, 5 min) and washed with water and acetone (5 times each). Then, the acetone and water in liquid phase was vaporized in an oven at 110 ºC.

Janus micromotor synthesis. 2 mL of the functionalized quantum dots were dissolved in 8 mL of 10% sodium dodecyl sulfate (cat. 71727) solution and placed in an erlenmeyer flask under vigorous stirring. Next, 1 mL of a chloroform (cat. 650498) containing 100 mg of polycaprolactone (cat. 440752), and 5 mg of platinum nanoparticles was rapidly added. The solution was stirred for 10 min and dropped onto a clean petri dish to enable evaporation of the chloroform and polymer solidification for 12 h. Micromotors were released from the petri dish by gentle pipetting and filtered through 12 µm pore size PC membranes. The microsensors (~20 µm) can be stored up to 2 months in an opaque vial without any changes in its properties.

RESULTS AND DISCUSSION

Figure 1A illustrate the *"ON-OFF"* fluorescence switching approach for the fast and selective detection of enterobacterial contamination. Initially, the micromotor display a strong fluorescent emission (see ON microscopy image). The motion-accelerated binding of LPS from *Salmonella enterica* selectively quenches the native fluorescent emission of the micromotors (see the absence of fluorescent emission in LPS/OFF image). Yet, under the presence of interfering saccharides (glucose, fructose and galactose) negligible fluorescent quenching is noted. The Janus microsensors act here as multifunctional vehicles, transporting the sensing probes and inducing an enhanced mixing effect for ultrafast detection, avoiding sample preparation and viscosity constraints (see Figure 1B). Optical images reveal the distribution of catalytic platinum nanoparticles on one size of the micromotor body and Janus structure. In addition, Raman spectra characterization reveals the successful incorporation of the quantum dots probes in the micromotor body (in green). Barret–Joyner–Halenda (BJH) pore-size distributions as well as Brunauer–Emmett–Teller (BET) surface areas studies further reveals the micro/mesoporous pore distribution (pore size <50 nm) nature of the micromotor, with BET surface areas of 1.36 and 0.0884 $m^2\ g^{-1}$ for the micromotor and the polymer, respectively. Such result indicates the inherent porous structure of the micromotor for further LPS diffusion and subsequent fluorescence quenching.[11]

As show in Figure 1C, the "enterobacterial test" can be simply performed by placing 1 µL of sample on the top of the microscope objective and a known amount of micromotors. Upon peroxide addition, the QDs probes -modified with 3-aminophenylboronic acid, PABA- binds to the target LPS, turning the fluorescent "OFF". Such changes can be easily monitored with the optical microscope, holding thus considerable promise for developing future portable detection schemes. The sensing principle, as illustrated in Figure 1D, rely on the specific interaction of the PABA groups in the GQDs with the KDO residue in the LPS core. As KDO possesses an acyclic 1,2-diol on the exocyclic side chain, it can selectively bind to PABA through reversible boronate formation, leading to a covalent cross-linked QDs structure by covalent anchored LPS. Such covalent cross-linking results in the generation of surface states for efficient fluorescence quenching that obeys the Lineweaver–Burk equations via surface quenching states.[11]

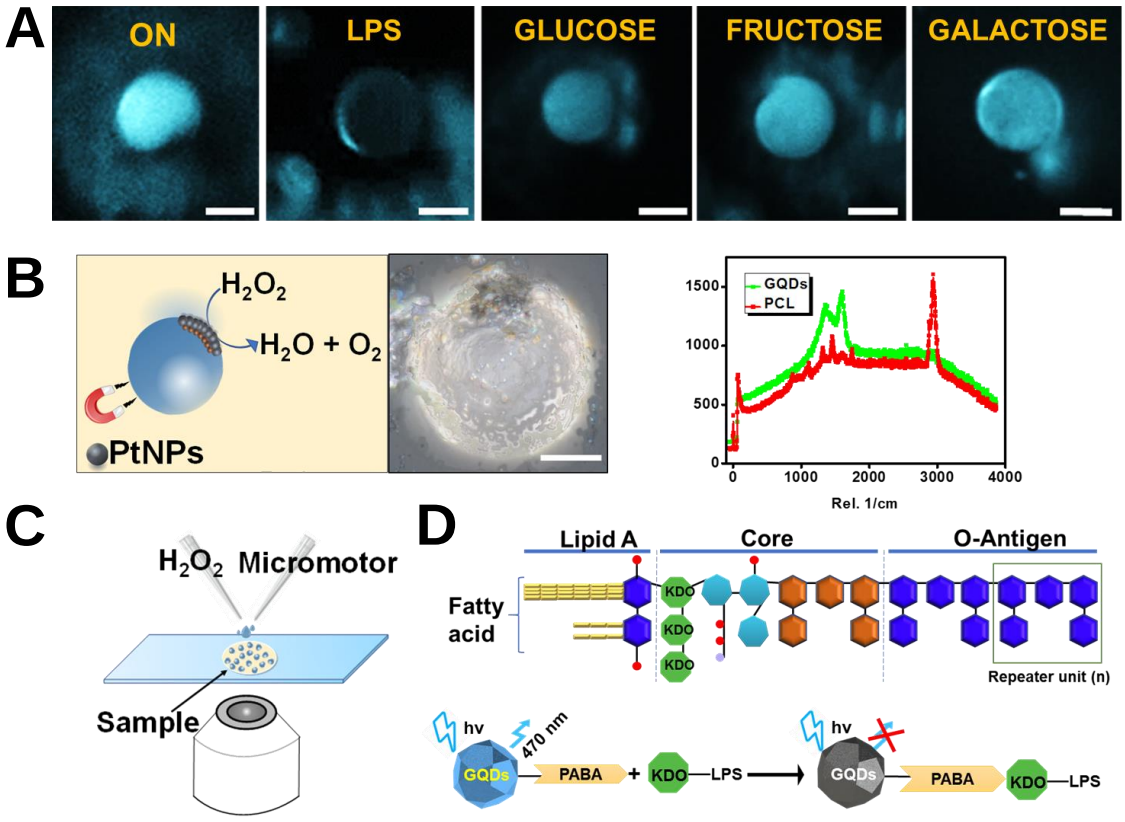

Figure 1. Self-propelled Janus microsensors for the detection LPS from *Salmonella enterica* (serotype enteritidis). (A) Real-time optical visualization of the LPS recognition event: time lapse fluorescent images of the micromotors before (ON) and after LPS addition (OFF) and selectivity of the protocol in the presence of interfering saccharides (see Videos S1 and S2). (B) Schematic of the microsensor operation and characterization. Optical images and Raman mapping showing the distribution of nanoparticles, GQDs and polycaprolactone (PCL) in the microsensor and corresponding Raman spectra. (C) Schematic of the set-up for the Janus micromotors based sensing protocol. (D) Schematics for structure of the LPS from *Salmonella enterica* and mechanism of quenching by LPS union to the quantum dot (GQDs) recognition units contained in the microsensors. Experimental conditions: 15 % H_2O_2, surfactant, 5% (w/v) sodium cholate. Scale bars, 20 μm. (Reviewer 2, comments 3 and 4)

Prior to demonstrate the practical utility of our Janus micromotor sensing approach in food samples, we evaluated the response time under different mixing and static conditions, as illustrated in Figure 2. The time lapse microscopy images and the corresponding fluorescence decay plot vs. time profile indicated that the quenching rate increased with time, until complete fluorescence quenching was achieved after 15 min navigation in solutions contaminated with 1 ng mL^{-1} of the LPS. Comparable results were obtained in an additional control experiment but using a magnetic stirring instead (ca. 200 rpm) to agitate the mixture. Yet, the autonomous bubble propulsion of the micromotors enable a great reduction of the amount of sample (1 μL), whereas for magnetic stirring 1 mL of the sample was required (1000-fold) thus indicating the crucial role of the enhanced fluid motion of the micromotors. This is further reflected by control experiments using static micromotors, which did not show any fluorescence quenching after 30 min interaction with LPS. To ensure adequate operation time for further experiments, the time between fuel addition and video acquisition was set to 15 min. In our previous work,[11] a response time of 5 min was obtained for LPS from *Escherichia Coli* detection. Such differences in the response time can be attributed to different diffusion profiles of the toxin into the micromotors due to the inherent differences in its structure. This is particularly promising for future multiplexing detection schemes, in which the micromotors can be functionalized with quantum dots -modified with different receptors for other specific target in the LPS molecule- with different emission wavelengths, allowing for a time-based endotoxin discrimination.

Next, we evaluated the effect of different LPS concentrations upon detection efficiency. Figure 3A display images of different micromotors navigating in solutions containing increased concentrations of LPS (up to 3.5 ng mL^{-1}), along with 15% of the peroxide fuel. The corresponding plot of fluorescence intensity (calculated as corrected fluorescence) vs. LPS concentration displays linear dependence up to 1 ng mL^{-1}, followed by a slight curvature, with nearly 100% fluorescence quenching at 3.5 ng mL^{-1}. The limits of detection and quantification were 0.07 and 0.20 ng mL^{-1}, respectively. Such concentrations are well below the level of LPS considered toxic to humans (275 μg mL^{-1})[3], which testified the applicability of our test to detect the presence of enterobacteria in food.

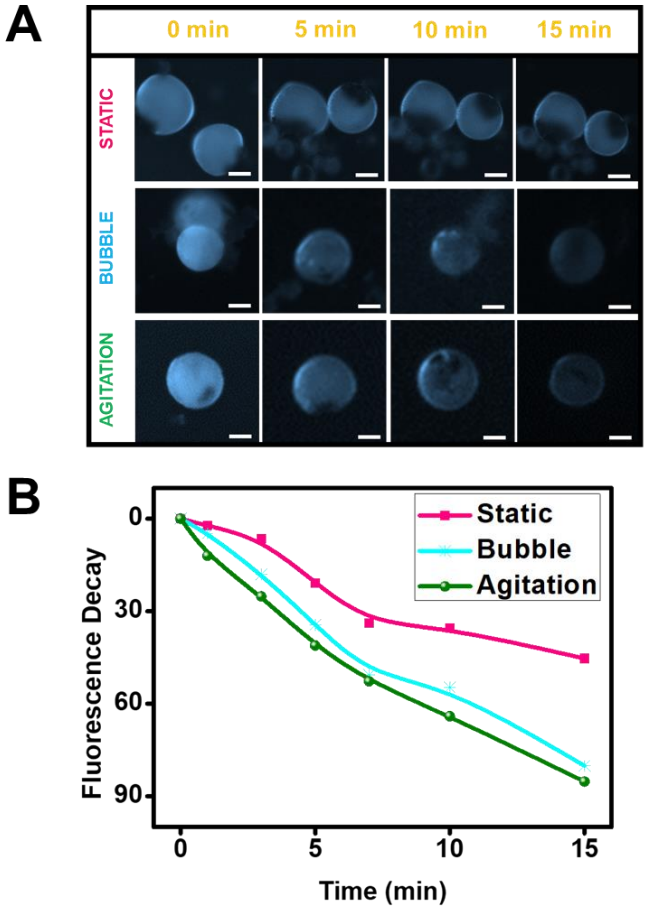

Figure 2. Response time of the Janus microsensors. (A) Time-lapse fluorescent images taken before and after the micromotor had navigated in a solution containing 1 ng mL^{-1} of LPS at different times and corresponding control experiments using external magnetic agitation. (B) Plot showing the fluorescence decay of the micromotors as a function of time at each condition. Experimental conditions: 15 % H_2O_2, surfactant, 5% (w/v) sodium cholate. Scale bars, 20 μm.

The practical utility of the micromotors was then demonstrated by their ability to detect the target LPS in unprocessed, fat rich and viscous food samples. The time lapse microscopy images of Figure 4A illustrate the efficient navigation and effective fluorescent quenching of the micromotors in milk, mayo, egg yolk and egg white samples previously contaminated with 1 ng mL^{-1} of endotoxin. The high viscosity and complexity of the samples result in a drastic decrease in the micromotor speed from 452 μm s^{-1} in water to 60, 58, 162 and 221 μm s^{-1} in milk, mayo, egg yolk and egg white, respectively. Yet, such speed decrease does not hamper the practical application of the micromotors since percent recoveries from 90 to 100 % were obtained (Figure 4B). Yet, the relatively low recoveries in fortified mayo and egg white samples (70 %) -due to its inherent complexity- do not hamper its practical application since excellent recovery reproducibility is still obtained.

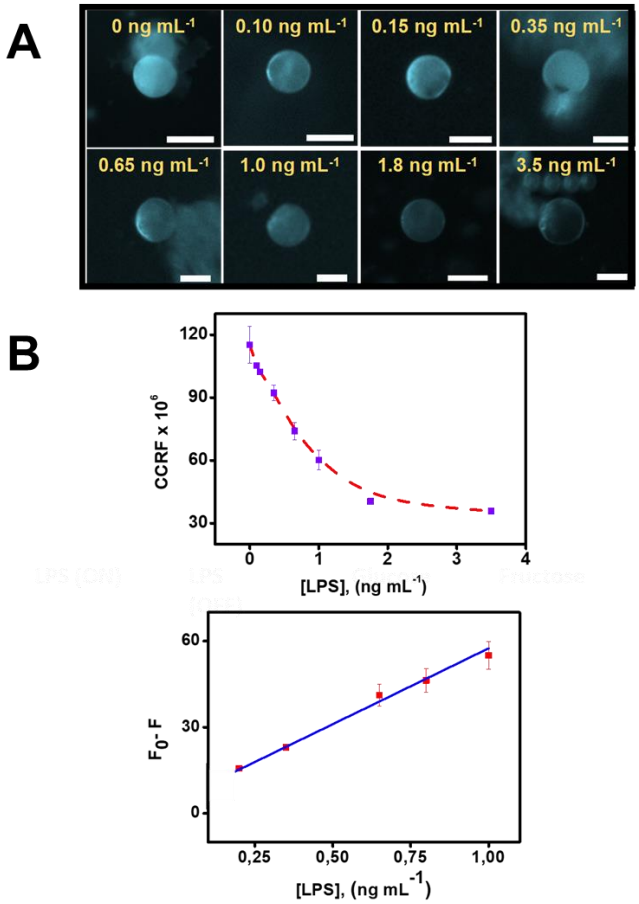

Figure 3. Dependence of the fluorescence quenching of Janus micromotors on LPS from *Salmonella enterica* concentrations. (A) Time-lapse images taken after the microsensors had navigated for 15 min in a solution containing 15% peroxide and increasing concentrations of LPS. (B) Plot showing the fluorescence quenching (as CCRF) of the micromotors and corresponding linear relationship. Scale bars, 20 μm. Error bars represent the standard deviation of 5 measurements (n = 5). Experimental conditions: 15 % H_2O_2, surfactant, 5% (w/v) sodium cholate. Scale bars, 20 μm.

CONCLUSIONS

In conclusion, we have developed here a powerful *"ON-OFF"* fluorescence sensing approach for the detection of *Salmonella enterica* endotoxin as main indicator of food contamination. The main advantage over bacteria culture or whole bacteria detection schemes is that early detection of food contamination (within minutes) can be achieved since endotoxins are released during bacteria growing. Continuous mixing induced by the motion and bubble-ejection mechanism across a contaminated sample results in a greatly enhanced mass transport, increasing the reaction rates between endotoxin and micromotors. The micromotor assay can readily detect a concentration as low as 0.07 ng mL^{-1} of LPS, which is far below the level considered toxic to humans (275 μg mL^{-1}). The high towing force of the Janus microsensors allow for the detection of LPS in unprocessed milk, egg and mayo samples in 15 minutes compared to several hours required by existing methods.[30] For example, the limulus amebocyte lysate (considered as the gold standard) requires at least 24 h to obtain reliable results. This is particularly attractive to avoid cumbersome sample preparation procedures and contamination risks. Also, the limit of detection provided by our

method (0.07 ng mL^{-1}) is superior or comparable to that provided by FRET-based sensors for LPS (0.1-3 µM),[31] aptamer-functionalized electrochemical sensors (0.01-1 ng mL^{-1}),[32] affinity-peptide based biosensors (130 pM)[33] or nanoMIP biosensors (0.44-50 ng mL^{-1}).[34] Yet, the above-mentioned sensors requires the use of expensive or labile biological recognition elements, which is a clear advantage of our method. The new micromotor-based fluorescent detection is particularly promising for food safety assurance and security biodefense applications against the use of bacteria toxins. Future multiplexing detection schemes can be achieved using micromotors functionalized with quantum dots probes modified with different receptors to other specific target in the LPS molecule with different emission wavelengths and a time-based endotoxin discrimination. Current efforts in our lab are aimed at the application of our micromotor strategy in real bacteria samples towards establishing the correlation of the number of bacteria vs. endotoxin concentration. Yet, more efforts are still needed to integrate our strategy into portable detection schemes *i.e.* microscope into a mobile phone.

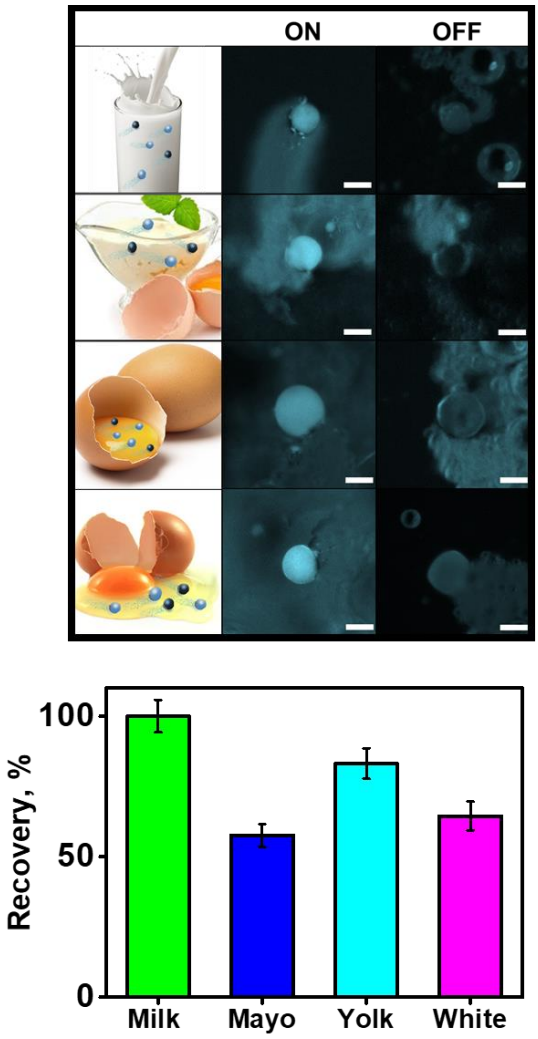

Figure 4. LPS detection on food samples (A) Time-lapse images of the microsensors (taken from Videos S3 and S4) in milk, mayo, egg yolk and egg white samples contaminated LPS from *Salmonella enterica* taken after the microsensors had navigated for 0 and 15 min in the contaminated solution. (B) Plot showing the average LPS recoveries in the different samples. Experimental conditions: 15 % H_2O_2, surfactant, 5% (w/v) sodium cholate. Scale bars, 20 µm. Error bars represent the standard deviation of 5 measurements (n = 5). Samples were fortified with 1 ng mL^{-1} of endotoxin.

ASSOCIATED CONTENT

Supporting Information

The Supporting Information is available free of charge on the ACS Publications website.

Supporting Figures (.pdf)

Supporting Video 1. Autonomous motion (linear and circular patterns) and effective fluorescence quenching of GQDs Janus micromotors in water before and after endotoxin from *Salmonella Enterica* addition (.avi)

Supporting Video 2. Selectivity of the GQDs Janus micromotors upon the presence of glucose, fructose and galactose vs. endotoxin (.avi)

Supporting Video 3. Efficient micromotors propulsion and endotoxin detection in milk and mayo samples (.avi)

Supporting Video 4. Efficient micromotors propulsion and endotoxin detection in egg yolk and egg white samples (.avi)

AUTHOR INFORMATION

Corresponding Author

* alberto.escarpa@uah.es

* beatriz.jurado@uah.es

Author Contributions

The manuscript was written through contributions of all authors. All authors have given approval to the final version of the manuscript

ACKNOWLEDGMENT

M. Pacheco acknowledges the University of Alcala for her FPI contract and the Spanish Ministry of Education for her FPU fellowship (FPU16/02211). B. J-S acknowledges support from the Spanish Ministry of Economy and Competitiveness (Ramon y Cajal contract, RYC-2015-17558, co-financed by EU) and from the University of Alcalá (Proyectos para la Creación y Consolidación de Grupos, Plan Propio UAH, CCGP2017-EXP/040). AE acknowledges financial support from the Spanish Ministry of Economy and Competitiveness (CTQ2014-58643-R and CTQ2017-86441-C2-1-R) and the NANOAVANSENS program (S2013/MIT-3029) from the Community of Madrid. The authors want to thank Mr. Jaime Rojo for his assistance during micromotors preparation.

REFERENCES

(1) Farahi, R. H.; Passian, A.; Tetard, L.; Thundat, T. *ACS Nano* **2012**, *6*, 4548-4556.
(2) de Jong, B.; Ekdahl, K. *BMC Public Health* **2006**, *6*, 4.

(3) Wang, A.; Molina, G.; Prima, V.; K.W. Wang, K. *J. Microbial Biochem. Technol*. **2011**, *03*, 2629.
(4) Pashazadeh, P.; Mokhtarzadeh, A.; Hasanzadeh, M.; Hejazi, M.; Hashemi, M.; de la Guardia, M. *Biosens. Bioelectron*. **2017**, *87*, 1050-1064.
(5) Coburn, B.; Grassl, G. A.; Finlay, B. B. *Immunol. Cell. Biol*. **2007**, *85*, 112-118.
(6) Lee, K. M.; Runyon, M.; Herrman, T. J.; Phillips, R.; Hsieh, J. *Food Control* **2015**, *47*, 264-276.
(7) Chen, S.; Zhao, S.; McDermott, P. F.; Schroeder, C. M.; White, D. G.; Meng, J. *Mol. Cell. Probes* **2005**, *19*, 195-201.
(8) Uyttendaele, M.; Vanwildemeersch, K.; Debevere, J. *Lett. Appl. Microbiol*. **2003**, *37*, 386-391.
(9) Sheikhzadeh, E.; Chamsaz, M.; Turner, A. P.; Jager, E. W.; Beni, V. *Biosens. Bioelectron*. **2016**, *80*, 194-200.
(10) Yan, X.; Li, W.; Liu, K.; Deng, L. *Anal. Meth*. **2015**, *7*, 10243-10250.
(11) Jurado-Sánchez, B.; Pacheco, M.; Rojo, J.; Escarpa, A. *Angew. Chem. Int. Ed*. **2017**, *56*, 6957-6961.
(12) Katuri, J.; Ma, X.; Stanton, M. M.; Sánchez, S. *Acc. Chem. Res*. **2017**, *50*, 2-11.
(13) Mei, Y.; Huang, G.; Solovev, A. A.; Ureña, E. B.; Mönch, I.; Ding, F.; Reindl, T.; Fu, R. K. Y.; Chu, P. K.; Schmidt, O. G. *Adv. Mater*. **2008**, *20*, 4085-4090.
(14) Mei, Y.; Solovev, A. A.; Sanchez, S.; Schmidt, O. G. *Chem. Soc. Rev*. **2011**, *40*, 2109-2119.
(15) Ozin, G. A.; Manners, I.; Fournier-Bidoz, S.; Arsenault, A. *Adv. Mater*. **2005**, *17*, 3011-3018.
(16) Paxton, W. F.; Kistler, K. C.; Olmeda, C. C.; Sen, A.; St. Angelo, S. K.; Cao, Y.; Mallouk, T. E.; Lammert, P. E.; Crespi, V. H. *J. Am. Chem. Soc*. **2004**, *126*, 13424-13431.
(17) Solovev, A. A.; Mei, Y.; Bermúdez Ureña, E.; Huang, G.; Schmidt, O. G. *Small* **2009**, *5*, 1688-1692.
(18) Wang, J. Nanomachines: Fundamentals and Applications, *Wiley-VCH* **2013**, *ISBN: 978-3-527-33120-8*.
(19) Bouffier, L.; Zigah, D.; Adam, C.; Sentic, M.; Fattah, Z.; Manojlovic, D.; Kuhn, A.; Sojic, N. *ChemElectroChem* **2014**, *1*, 95-98.
(20) Jurado-Sanchez, B.; Escarpa, A.; Wang, J. *Chem. Commun*. **2015**, *51*, 14088-14091.
(21) Jurado-Sánchez, B.; Wang, J.; Escarpa, A. *ACS Appl. Mater. Interfac*. **2016**, *8*, 19618-19625.
(22) Sentic, M.; Arbault, S.; Goudeau, B.; Manojlovic, D.; Kuhn, A.; Bouffier, L.; Sojic, N. *Chem. Commun*. **2014**, *50*, 10202-10205.
(23) Singh, V. V.; Kaufmann, K.; Orozco, J.; Li, J.; Galarnyk, M.; Arya, G.; Wang, J. *Chem Commun*. **2015**, *51*, 11190-11193.
(24) Jurado-Sánchez, B.; Escarpa, A. *Trends Anal. Chem*. **2016**, *84*, 48-59.
(25) Wang, J. *Biosens. Bioelectron*. **2016**, *76*, 234-242.
(26) Esteban-Fernández de Ávila, B.; Martín, A.; Soto, F.; Lopez-Ramirez, M. A.; Campuzano, S.; Vásquez-Machado, G. M.; Gao, W.; Zhang, L.; Wang, J. *ACS Nano* **2015**, *9*, 6756-6764.
(27) Maria-Hormigos, R.; Jurado-Sánchez B.; Escarpa, A. *Adv. Func. Mater*. **2017**, DOI: 10.1002/adfm.201704256.
(28) Molinero-Fernández, A.; Moreno, M.; Lopez, M. A.; Escarpa, A. *Anal. Chem*. **2017**, *89*, 10850-10857.
(29) Srivastava, S. K.; Schmidt, O. G. *Chem. Eur. J*. **2016**, *22*, 9072-9076.
(30) Jarvis, W. R.; Highsmith, A. K. *J. Clin. Microbiol*. **1984**, *19*, 17-20.
(31) Voss, S.; Fischer, R.; Jung, G.; Wiesmuller, K. H.; Brock, R. *J. Am. Chem. Soc*. **2007**, *129*, 554-561.
(32) Kim, S. E.; Su, W.; Cho, M.; Lee, Y.; Choe, W. S. *Anal. Biochem*. **2012**, *424*, 12-20.
(33) Lim, S. K.; Chen, P.; Lee, F. L.; Moochhala, S.; Liedberg B. *Anal. Chem*. **2015**, *87*, 9408-9412.
(34) Altintas, Z.; Abdin, M. J.; Tothill, A. M.; Karim, K.; Tothill, I. E. *Anal. Chim. Acta* **2016**, *935*, 239-248.